



MIT Open Access Articles

Efficient Light Trapping in Inverted Nanopyramid Thin Crystalline Silicon Membranes for Solar Cell Applications

The MIT Faculty has made this article openly available. **Please share** how this access benefits you. Your story matters.

Citation	Mavrokefalos, Anastassios, Sang Eon Han, Selcuk Yerci, Matthew S. Branham, and Gang Chen. "Efficient Light Trapping in Inverted Nanopyramid Thin Crystalline Silicon Membranes for Solar Cell Applications." Nano Lett. 12, no. 6 (June 13, 2012): 2792–2796.
As Published	http://dx.doi.org/10.1021/nl2045777
Publisher	American Chemical Society (ACS)
Version	Author's final manuscript
Citable link	http://hdl.handle.net/1721.1/86899
Terms of Use	Article is made available in accordance with the publisher's policy and may be subject to US copyright law. Please refer to the publisher's site for terms of use.

Efficient Light-Trapping in Inverted Nano-Pyramid Thin Crystalline Silicon Membranes for Solar Cell Applications

*Anastassios Mavrokefalos, Sang Eon Han, Selcuk Yerci, Matthew S. Branham and Gang Chen**

Department of Mechanical Engineering, Massachusetts Institute of Technology, 77 Massachusetts
Avenue, Cambridge MA 02139, USA.

AUTHOR EMAIL ADDRESS: *gchen2@mit.edu

RECEIVED DATE (to be automatically inserted after your manuscript is accepted if required according to the journal that you are submitting your paper to)

ABSTRACT: Thin-film c-Si solar cells with light-trapping structures can enhance light absorption within the semiconductor absorber layer and reduce material usage. Here we demonstrate that an inverted nano-pyramid light-trapping scheme for c-Si thin films, fabricated at wafer-scale via a low-cost wet etching process, significantly enhances absorption within the c-Si layer. A broadband enhancement in absorptance that approaches the Yablonovitch limit¹ is achieved with minimal angle dependence. We also show that c-Si films less than 10 μm in thickness can achieve absorptance values comparable to that of planar c-Si wafers thicker than 300 μm that amounts to an over 30-fold reduction in material usage. Furthermore the surface area increases by a factor of only 1.7, which limits surface recombination losses in comparison with other nanostructured light-trapping schemes. These structures will not only significantly curtail both the material and processing cost of solar cells, but also achieve the high

efficiency required to enable viable c-Si thin-film solar cells in the future.

KEYWORDS. Light trapping, Photovoltaics, Optical absorption, Inverted pyramids, Thin film solar cells.

MANUSCRIPT TEXT:

Bulk c-Si solar cells dominate the photovoltaic (PV) market. Typically, c-Si wafers 180-300 μ m thick are used to ensure adequate absorption of sunlight, and this material accounts for about half of the total module cost.^{2, 3} In bulk crystalline Si solar cells, light-trapping is typically provided by randomly textured surfaces.⁴ The characteristic size of these textures is typically 3-10 μ m, which is much larger than the wavelength of sunlight and not applicable for thin films. Thus various nanophotonic structures have been studied in recent years, including nanowires, nanoholes, nanocones, plasmonic particles, and photonic crystal surface structures.⁵⁻¹⁴ The efficiency of Si nanowire and nanohole-based solar cells^{6, 7, 15-17} has been limited to \sim 10%, a value far smaller than the \sim 25% efficiency for state-of-the-art thick c-Si solar cells.¹⁸ One major reason for the low efficiency in solar cells with nanowires and nanoholes is the high surface recombination rates due to the large surface area, which is usually more than an order of magnitude larger than flat cells.¹⁹ It was recently reported that flat 10-20 μ m thick c-Si based solar cells can have conversion efficiencies up to 15%.^{20, 21} Our previous investigation into nano-pyramid structures has shown great promise to enhance light absorption in thin c-Si based solar cells while minimizing the surface area increase, but this was limited to simulation. In this paper, we experimentally show that c-Si thin-films with thicknesses less than 10 μ m can absorb as well as 300 μ m-thick flat c-Si substrates when they are decorated with inverted nano-pyramid structures.

We recently investigated various light-trapping structures based on crystalline Si materials such as nanowires, nanoholes, pyramids, and inverted pyramids through numerical simulation.²²⁻²⁴ Of all these structures, inverted nano-pyramids possess three major advantages for experimental demonstration: (1) they enable films that are less than 10 μ m-thick to achieve similar efficiencies to bulk c-Si cells with a

thickness $>300\mu\text{m}$, (2) the surface area increase is only 1.7 times compared to flat surfaces, which minimizes surface recombination losses, and (3) the fabrication of the structures is easy and cost-effective.

We fabricated inverted nano-pyramids using standard scalable microfabrication techniques based on interference lithography (IL)²⁵ and wet Si etching²⁶. Figure 1(a) shows an optical image of the typical sample. The exposed area is limited by the exposure area of the IL tool to approximately $25\text{mm} \times 25\text{mm}$. It should be noted that IL can be applied to standard $156\text{mm} \times 156\text{mm}$ wafers.²⁷ Typical scanning electron microscope (SEM) images of the resulting structures are illustrated in Figs. 1(b) and (c). Figure 1(b) illustrates the top-view of inverted nano-pyramids with a periodicity of 700nm and a mean separation of 100nm between the pyramids produced after etching in a potassium hydroxide (KOH) solution. Figure 1(c) illustrates the cross sectional SEM of the resulting structure with the insets clearly showing the interfaces of the SiN_x , Si, SiO_2 and Ag layers. The sample illustrated here employed a 90nm thick SiN_x , $10\mu\text{m}$ thick Si, $1\mu\text{m}$ thick SiO_2 , and 200nm thick Ag as antireflection coating, active absorbing medium, surface passivation and back-reflector, respectively. Because of the anisotropic etching of c-Si in the KOH solution, inverted nano-pyramids are formed at an angle of 54.7 degrees to the wafer surface, which is responsible for the factor of 1.7 increase in surface area.

We carried out absorption measurements for the structure shown in Fig. 1 using a spectrophotometer attached to an integrating sphere. Figure 2(a) shows the experimental results measured at 8 degrees from the surface normal compared to the simulated results at 10 degrees. Simulations were carried out using the transfer matrix method.²⁸ The experimental results show good agreement with the theoretical predictions over almost the entire spectrum. The deviations at short wavelengths are most likely due to the variation in the separation distance between pyramids (ridge size). Samples with different ridge size variations yielded absorptance fluctuations that are most pronounced at short wavelengths. Close up SEM images showed that the separation between successive pyramids is approximately 100nm with fluctuations of $\sim 10\text{nm}$ for the sample shown in Fig. 1. Furthermore, the thickness variations of the SiN_x

layer deposited on inverted nano-pyramids limit simulation of the exact structure. As a baseline, we also measured the absorptance of a flat 10 μm Si film coated with a 70nm SiN_x anti-reflection coating. The film with inverted nano-pyramids shows a clear absorption enhancement throughout the solar spectrum compared to the flat film, demonstrating the light-trapping benefit of inverted nano-pyramids. Moreover, based on the calculations we found that absorption in the silver layer is negligible compared to absorption in Si as shown in Fig. 2. The absorptance of thin-film c-Si layer with inverted nano-pyramids is close to the Yablonovitch limit, confirming the effectiveness with which they trap photons. Absorption in periodic surface structures can indeed exceed the Yablonovitch limit for a particular angle of incidence, but not in the case of isotropically incident radiation.¹³ The calculations are performed for wavelengths up to 1.1 μm , which corresponds to the band gap of c-Si.

We also fabricated inverted nano-pyramids using a 5 μm -thick c-Si film with an average ridge size of 50nm and measured the absorption spectrum as shown in Fig. 2(b). The experimental absorptance matches well with theoretical predictions; the variations at short wavelengths can be attributed to the same effects as described earlier for 10 μm -thick films.

To fully gauge optical absorption enhancement we calculated the maximum photovoltaic efficiency η , following the treatment developed by Shockely and Queisser²⁹, of our structures based on the calculated and measured absorptance in the Si films. This is the efficiency of a photovoltaic cell at room temperature when only radiative recombination of charge carriers occurs among other mechanisms. We assumed that the radiation intensity due to carrier recombination is Lambertian and constructed its angular dependence based on the radiation intensity in the surface normal. In the calculations, AM1.5G solar flux³⁰ was used for incident light. Experimental and theoretical maximum efficiency values are plotted in Fig. 3 for (1) 5 and 10 μm films with inverted nano-pyramids presented earlier (experiment), (2) 10 μm and 300 μm flat films (experiment), and (3) 5 and 10 μm -thick films consisting of inverted nano-pyramids with a ridge separation of 50 and 100nm respectively (theory). Additionally, theoretical maximum efficiency curves are plotted as a function of thickness for a flat film and a film with inverted

nano-pyramids with no ridge spacing. Also plotted in the figure is the Shockley-Queisser limit assuming all incident photons above the bandgap is absorbed. For the experimental results, we obtained the absorptance of the silicon layer by subtracting the calculated absorptance in Ag from the total measured absorptance. The calculated absorptance in Ag is based on the measured dielectric function of the deposited Ag layer obtained using ellipsometry. There is excellent agreement between the experimental data and the theoretical curves for both inverted nano-pyramids and flat films as shown in Fig. 3. The small difference between theory and experiment for the absorptance of inverted nano-pyramids can be related to the $\sim 10\text{nm}$ variation in ridge separation as noted earlier. The effect of a 10nm variation in ridge size is more pronounced for the film with a 50nm ridge gap than for the one with a 100nm ridge gap because of the proportionally greater variation in the ridge width. Based on the maximum efficiency measurements and calculations, the 5 and $10\mu\text{m}$ -thick films with inverted nano-pyramids can absorb light with efficiencies similar to those of planar films that are $300\mu\text{m}$ thick. Therefore, inverted nano-pyramids can yield an order of magnitude reduction of silicon mass.

Figure 4 illustrates the measured and simulated angular dependence of maximum efficiency for the structure demonstrated in Fig. 1. We can clearly see that the theoretical maximum efficiency is almost independent of the angle of incidence up to 40 degrees and is validated by our experiments. The inset shows the angular dependence of absorptance for the structure shown in Fig. 1 taken with a variable angle attachment in the integrating sphere (see method).

Finally, Figure 5 shows what the expected short circuit current would be for each one of our experimental structures, based on 100% internal quantum efficiency (i.e. every photon that is absorbed will contribute to the current of the cell in short-circuit mode). The short circuit current of 37.5 mA/cm^2 for the $10\mu\text{m}$ and 37.1 mA/cm^2 for the $5\mu\text{m}$ thick samples with inverted nano-pyramid structures are close to their respective Yablonovitch limits values of 39.4 mA/cm^2 ($10\mu\text{m}$ thick) and 37.4 mA/cm^2 ($5\mu\text{m}$ thick). Furthermore they are significantly higher than the short current of 29.5 mA/cm^2 for $10\mu\text{m}$ thick flat film with optimized anti-reflection coating and comparable to the value of 37.2 mA/cm^2 for

the 300 μm thick flat film with optimized anti-reflection coating.

In conclusion we experimentally and theoretically investigated the light-trapping properties of periodic inverted nano-pyramid structures on thin crystalline silicon films fabricated by a microfabrication process based on interference lithography. Through optical characterization, we demonstrated that inverted nano-pyramids significantly enhance light absorption above the silicon bandgap across the solar spectrum in thin crystalline silicon films with respect to planar films. This enhancement is almost independent of angle of incidence and approaches the Yablonovitch limit. Our work suggests that one can achieve solar cell efficiencies in c-Si thin films comparable to their bulk counterparts, enabling a reduction of silicon material usage by one order of magnitude.

Methods. *Inverted Nano-Pyramid fabrication.* The fabrication process flow is as follows; First, a commercial silicon-on-insulator (SOI) wafer was acquired with the desired Si and SiO₂ thicknesses. Then an array of holes was patterned in negative photoresist on the surface of the Si thin film using interference lithography (IL). Subsequent wet etching in an aqueous potassium hydroxide (KOH) solution was used to produce the inverted pyramids on the surface of the Si thin film and etch the backside of the Si handle wafer. KOH wet chemistry was chosen because it etches c-Si anisotropically yielding a self-aligned pyramid structure. Finally a SiN_x anti-reflection coating was deposited on top of the inverted pyramids with plasma enhanced vapor deposition (PECVD) and a silver layer was deposited by evaporation on the backside of the SiO₂ to simulate the Ag back contact of the photovoltaic module.

Optical Measurements. Integrated reflection measurements were carried out with a Perkin Elmer LAMBDA 950 UV/Vis/NIR Spectrophotometer System using a 150mm integrating sphere attachment. The Spectrophotometer uses a holographic grating monochromator with 1440 lines/mm UV/Vis blazed at 240 nm, 360 lines/mm NIR blazed at 1100 nm, a wavelength range from 175nm – 3300nm, and a 3-120mm spot height. The integrating sphere measures the total reflection (R) of the light incident on a surface, including both specular and diffuse components. Because the samples measured here have a Ag

metal layer on the back to prevent light transmission, the absorptance (A) of the final structure can be simply calculated from the $A=I-R$ where R is the reflectance. The measurement covered the solar spectrum that is useful for c-Si with a bandgap of 1.1 eV. The measurements of the angle dependence of absorptance were carried out using the variable angle center-mount option in which the sample is suspended in the middle of the sphere. Spectroscopic ellipsometry measurements were performed to obtain the thickness and optical constants of silicon nitride layers deposited on flat silicon films. The Δ and Ψ values were measured using a J. A. Woollam Co. variable-angle spectroscopic ellipsometer (VASE) in a spectral range 400-1200 nm. The silicon nitride data were analyzed using the Cauchy-Urbach model.³¹ Silver films deposited on SOI wafers were also analyzed by spectroscopic ellipsometry using the default model for Ag in the VASE library which yielded similar values for the refractive index and absorption coefficient of Ag compared to the values in the literature.³²

ACKNOWLEDGMENT. We thank T. Buonassisi and J. Sullivan at MIT for helping with the optical measurements. This research was supported by Nanoscale Science and Engineering Initiative of the National Science Foundation under NSF Award Number CMMI-0751621 through the Center for Scalable and Integrated Nanomanufacturing at U. C. Berkeley. A. Mavrokefalos is supported by the Post-doctoral fellowship in the Cyprus Institute Program for Energy Environment and Water Resources (CEEW) at the MIT Laboratory for Energy and the Environment (LFEE).

FIGURE CAPTIONS

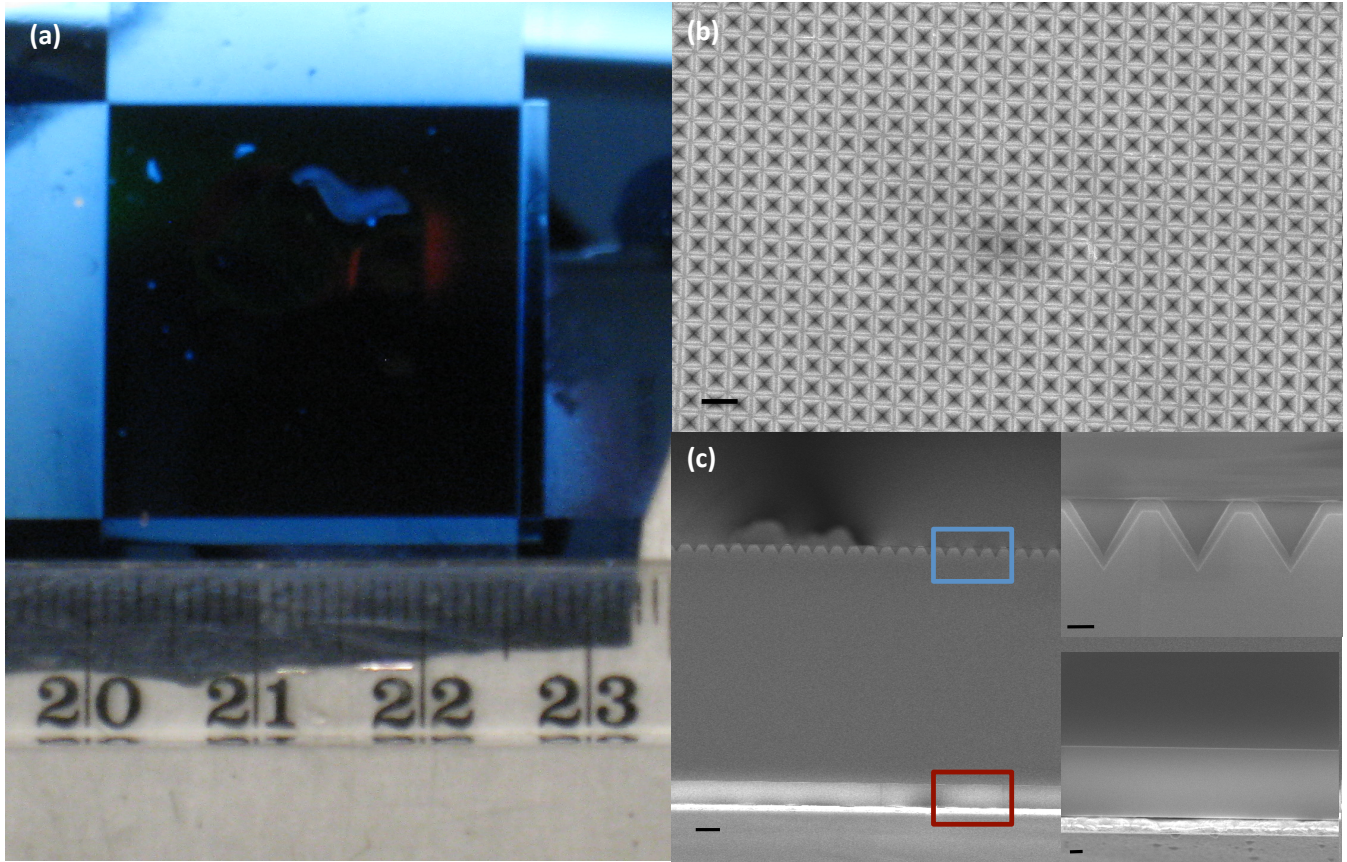


Figure 1: (a) Optical image, (b) Top view SEM image, and (c) Cross-sectional SEM image of the 10 μm c-Si film illustrating the patterned inverted nano-pyramids on a 700nm period. A 90nm SiN $_x$ layer is deposited on the inverted pyramids and a SiO $_2$ (1 μm) and a silver (200 nm) layer are at the backside of the c-Si film. The right bottom insets are close-ups of the blue and red boxed regions. The scale bars in both (b) and (c) are 1 μm . The scale bars in the insets in (c) are 200nm.

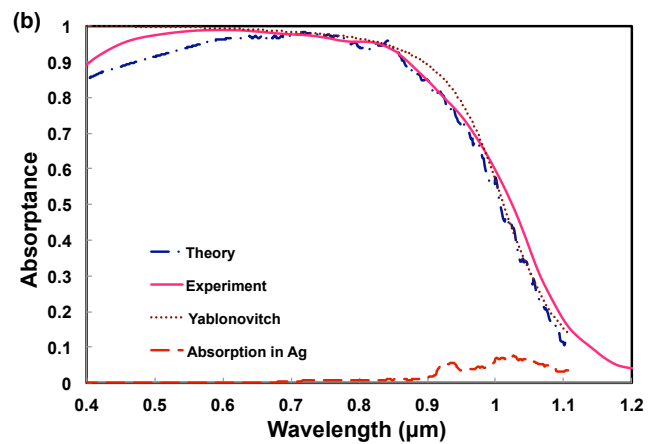
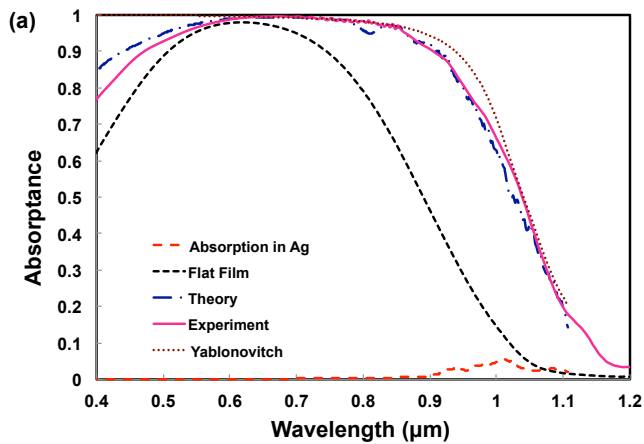


Figure 2: Comparison of the theoretical and experimental absorptance spectra, the Yablonovitch limit corresponding to the c-Si thickness, and the calculated absorptance in the Ag layer for film thicknesses of (a) 10 μm (the structure of Fig. 1) and (b) 5 μm , respectively. The experimental absorptance spectra for a flat film is included in (a) as a base line. The dimensions of the flat film structure are 70nm SiN_x, 10 μm Si, 250nm SiO₂ and 200nm Ag in thickness. In (b), the inverted pyramid structure consists of 90nm SiN_x, 5 μm Si, 0.5 μm SiO₂ and 200nm Ag. The Yablonovitch limit was obtained by considering a c-Si film on the SiO₂ and Ag layers of the same thickness as in the corresponding inverted pyramid structures. Note that, except for the Ag absorption curves, the other absorptance spectra account for absorption in all layers. For all the theoretical curves, the spectra were averaged over a wavelength range to smoothen sharp peaks.

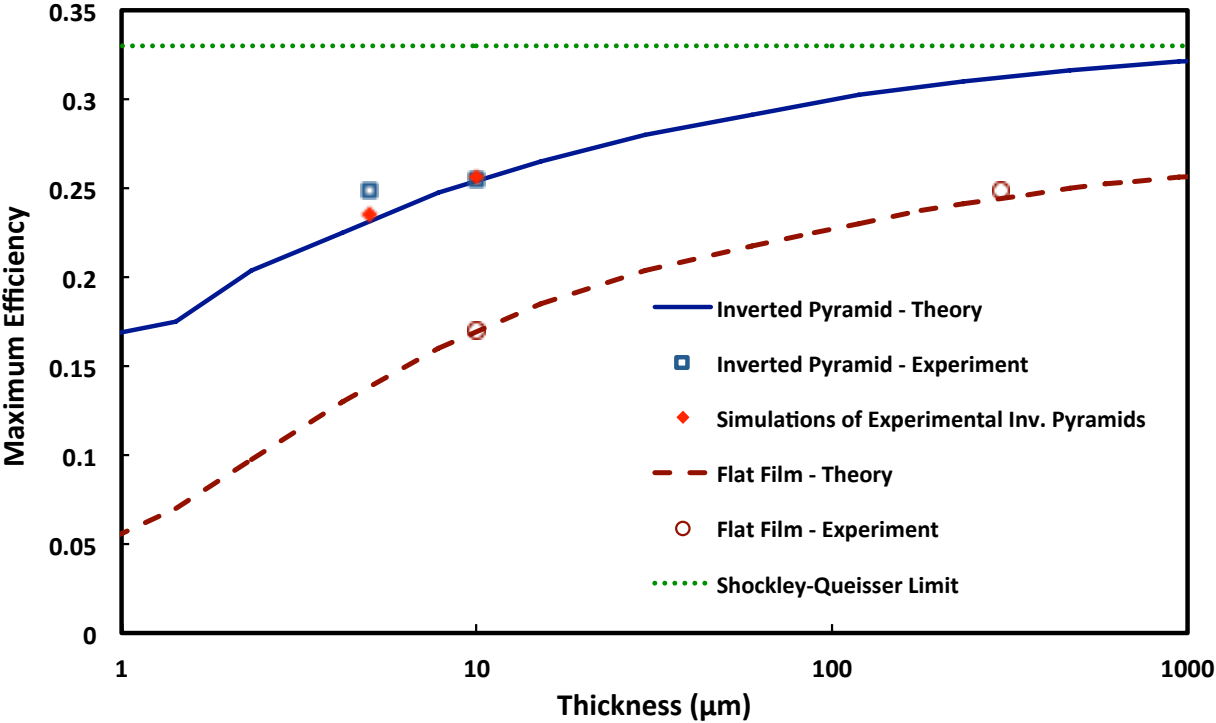


Figure 3: Maximum efficiency at normal incidence as a function of thickness for simulated inverted nano-pyramids (blue solid line) and a planar film (brown dashed line) with 90nm and 63nm SiN_x anti-reflection coatings, respectively. The blue open squares represent the experiments for inverted nano-pyramids and the brown open circles the experiments for flat films at 8 degrees incidence angle. The red

diamonds represent the simulated maximum efficiency for the structures used in experiments at the incidence angle of 10 degrees. The dotted green line is the maximum theoretical Shockley-Queisser efficiency. The experimental results were obtained by subtracting the calculated absorptance in Ag from the measured total absorptance, a small correction of less than 1% in maximum efficiency.

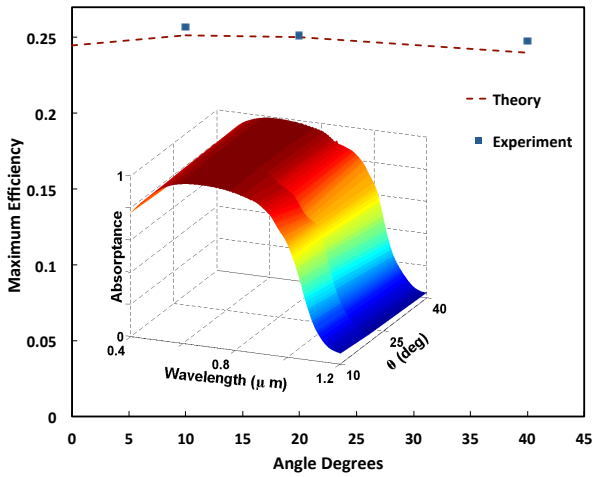


Figure 4: Comparison of experimental and simulated maximum efficiency for the structure shown in Fig. 1 at different incidence angles. Inset is the experimental light absorptance for the structure of Fig. 1 measured at incidence angles of 10, 20 and 40 degrees.

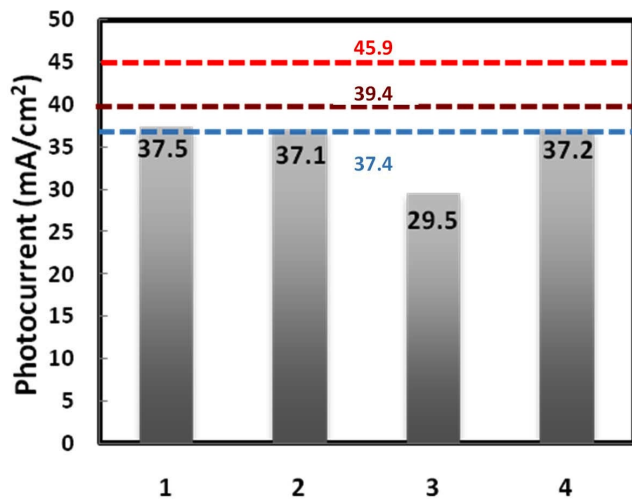


Figure 5: Comparison of the short circuit currents generated by our four structures (gray bars), the Yablonovitch limits for 5μm (blue dashed line) and 10μm (brown dashed line) thick silicon films, and full absorption in silicon (red dashed line).

REFERENCES.

- (1) Yablonovitch, E. *J. Opt. Soc. Am.* **1987**, 72, 899-907.
- (2) Green, M. A. *J. Mater. Sci.: Mater. Electron.* **2007**, 18, S15-S19.
- (3) Brendel, R. *Sol. Energy* **2004**, 77, 969-982.
- (4) Campbell, P.; Green, M. A. *J. Appl. Phys.* **1987**, 62, 243-249.
- (5) Kelzenberg, M. D. et al. *Nat. Mater.* **2010**, 9, 239-44.
- (6) Peng, K. Q. et al. *Small* **2005**, 1, 1062-1067.
- (7) Peng, K. Q.; Wang, X.; Li, L.; Wu, X. L.; Lee, S. T. *J. Am. Chem. Soc.* **2010**, 132, 6872-3.
- (8) Atwater, H.A.; Polman, A. *Nat. Mater.* **2010**, 9, 205-13.
- (9) Munday, J. N.; Atwater, H. A. *Nano Lett.* **2011**, 11, 2195-201.
- (10) Pillai, S.; Catchpole, K. R.; Trupke, T.; Green, M. A. *J. Appl. Phys.* **2007**, 101, 8.
- (11) Stuart, H. R.; Hall, D. G. *Appl. Phys. Lett.* **1996**, 69, 2327-2329.
12. Hsu, C. M.; Connor, S.T.; Tang, M. X.; Cui, Y. *Appl. Phys. Lett.* **2008**, 93, 133109.
- (13) Yu, Z. F.; Raman, A.; Fan, S.H. *Proc. Nat. Acad. Sci. U. S. A.* **2010**, 107, 17491-17496.
- (14) Cao L. et. a. *Nano Lett.* **2011**, 10, 439-445.
- (15) Tsakalacos, L. et al. *Appl. Phys. Lett.* **2007**, 91, 233117.
- (16) Muskens, O. L.; Rivas, J. G.; Algra, R. E.; Bakkers, E. P. A. M.; Lagendijk, A. *Nano Lett.* **2008**, 8, 2638-2642.
- (17) Garnett, E.; Yang, P. *Nano Lett.* **2010**, 10, 1082-1087.

- (18) Green, M. A. *Prog. Photovolt.* **2009**, 17, 183-189.
- (19) Kelzenberg, M. D. et al. *Energy & Environ. Sci.* **2011**, 4, 866-871.
- (20) Cruz-Campa, J. L. et al. *Sol. Energ. Mat. Sol.* **2011**, 95, 551-558.
- (21) Yoon, J. et al. *Nat. Commun.* **2011**, 2, 343.
- (22) Hu, L.; Chen, G. *Nano Lett.* **2007**, 7, 3249-52.
- (23) Han, S. E.; Chen, G. *Nano Lett.* **2010**, 10, 1012-5.
- (24) Han, S. E.; Chen, G. *Nano Lett.* **2010**, 10, 4692-6.
- (25) Savas, T. A.; Schattenburg, M. L.; Carter, J. M.; Smith, H. I. *J. Vac. Sci. Technol. B.* **1996**, 14, 4167-4170.
- (26) Kovacs, G. T. A.; Maluf, N. I.; Petersen, K. E. *Proc. IEEE* **1998**, 86, 1536-1551.
- (27) Mao, W.; Wathuthanthri, I.; Choi, C. H. *Opt. Lett.* **2011**, 36, 3176-3178.
- (28) Pendry, J. B.; Mackinnon, A. *Phys. Rev. Lett.* **1992**, 69, 2772-2775.
- (29) Shockley, W.; Queisser, H. J. *J. Appl. Phys.* **1961**, 32, 510-519.
- (30) *Air Mass 1.5 Spectra* [Online]; American Society for Testing and Materials, <http://rredc.nrel.gov/solar/spectra/am1.5/>.
- (31) Tompkins, H. G.; Gregory, R. B.; Deal, P. W.; Smith, S. M. *J. Vac. Sci. Technol. A.* **1999**, 17, 391-397.
- (32) *Handbook of Optical Constants of Solids*; Palik, E. D., Ed.; Academic: Orlando, FL, 1985.